Desalination and Water Treatment
www.deswater.com

doi: 10.5004/dwt.2020.25747

190 (2020) 412–423
June

Adsorptive removal of methylene blue by low-cost *Vibernum grandiflorum* (VG) leaves: kinetics and thermodynamic studies

Rashida Fiaz, Muhammad Hafeez*, Rashid Mahmood

Department of Chemistry University of Azad Jammu & Kashmir Muzaffarabad, Pakistan, emails: abrarashida@gmail.com (R. Fiaz), smhafeezkhan@yahoo.com (M. Hafeez), rashid_meh786@yahoo.com (R. Mahmood)

Received 20 July 2019; Accepted 15 February 2020

ABSTRACT

Viburnum grandiflorum (VG) leaves have been used for the Methylene Blue (MB) removal from its aqueous solution. The effect of contact time 10–100 min, initial concentration 5–25 mg/L, pH 4–13, temperature 293–323 K and biosorbent dosage 0.15–0.45 g was investigated. The maximum removal efficiency and adsorption capacity were calculated to be 95.59% and 7.96 mg/g for a sample having initial concentration 25 mg/L along with 0.45 g of adsorbent agitated for 60 min at 298 K and pH = 9. At optimized experimental conditions, the dye uptake capacity and percentage efficiency of base modified VG leaves were obtained to be 8.25 mg/g and 98%. By applying isotherm models such as Langmuir, Freundlich, and Temkin model, the observed data were found to be best fitted with Langmuir adsorption isotherm ($R^2 = 0.99$). The adsorption kinetic models such as pseudo-first-order, pseudo-second-order and Elovich were also applied for the adsorption of MB onto VG leaves. The experimental data best fitted to the pseudo-second-order model ($R^2 = 0.99$). The nature of adsorption was predicted by calculation of enthalpy ($\Delta H°$), free energy ($\Delta G°$) and entropy ($\Delta S°$) changes. The low $\Delta G°$ values (–17.417, –21.664 and –23.212 kJ/mol) 303, 313, and 323 K, respectively, showed that the process of adsorption was spontaneous. The MB loaded VG leaves can be best desorbed (25.78%) by using 0.1 M HCl. The VG leaves can be effective for the MB removal from aqueous solutions.

Keywords: Viburnum grandiflourm; Methylene Blue; Adsorption capacity; Removal efficiency

1. Introduction

Water pollution is the major environmental pollution caused by different sources such as domestic sewage, industrial wastes, urban, and agricultural runoff containing fertilizers, chemical contaminants, littering, eutrophication and pesticides. Industrial wastewater discharged into rivers, streams and channels containing colored dyes is the basic cause of water contamination. Dyes are obtained synthetically and they have a complex structure of aromatic molecules that are stable and less susceptible to bio-degradation. The toxic dyes of various kinds are encountered in sewage discharge from cosmetics, fabrics, printing, leather, plastics, rubber, paper, dye manufacturing and food handling industries [1,2]. Currently, there are 10,000 dyes in use with overall 700,000 metric tons yearly production worldwide and about 5%–10% of dye's material is emitted in industrial sewage waste [3]. The discharge of dyes from various industries causes water contamination, which acts as a severe source of environmental pollution [4]. Methylene blue (Basic dye) is highly water contaminating as compared to the anionic dyes [5]. Methylene blue (MB) dye is readily soluble in water and most commonly employed in dyeing cotton, leather, calico, pharmaceutical purposes, lithography and tannin [6]. This dye can cause irritation in skin and eyes as well as meticulous consequences such

---

* Corresponding author.

as blood variations in human beings [5,7]. MB can set off vomiting, sickness, diarrhea, plentiful sweating, mental disorder, suffocation, and gastritis [5]. Thus, a significance has been engrossed in eliminating such dyes from the wastewater discharges. Several techniques, such as inverse osmosis, ionic substitution, membrane sanitization, traditional coalescence, organic precipitation besides adsorption are commonly practiced in taking out dyes from surplus water [2,8]. The adsorption process is an appropriate and moderately admirable procedure on account of the ease of design, availability and capability in treating dyes at a minimum rate than former methods [5,8]. Activated carbons are commonly known for their great adsorption capacities towards an enormous amount of carbon-based/mineralized metallic ions. The activated carbon was avoided as an adsorbent due to high cost [9] therefore, the price effective adsorbents were introduced. Agricultural wastes or biomass are easily accessible in large amounts and can be effectively utilized as adsorbents in eliminating the dyes from different types of industrial wastewater [10]. Various forms of agrarian rubbish for example rinds of orange [11], *Hordeum vulgare* and hull [12,13], sawdust [14], fly ash [15,16], castor seed shell [17], pine cone [5] and cereal chaff [18] are being used to eliminate the methylene blue from wastewater. Many adsorbents such as wool fiber and cotton fiber [19], coconut coir [20], bagasse [21], *Parthenium hysterophorus* [22], rice husk [23], neem husk [24], tamarind fruit shell [25], silk cotton hull [26], tuberose sticks [27], tamarind fruit shell [28] and *Ficus palmata* leaves [29] are considered low-cost, very operative and safe. The current study was carried out to evaluate the *Viburnum grandiflorum* (VG) leaves (collected from Rairban, district Bagh Azad Jammu & Kashmir Pakistan) capacity in eliminating MB from the solution. The effects of temperature, initial dye concentration, pH, contact time on MB adsorption were also interpreted.

2. Experimental

2.1. Preparation of standard solution

Methylene blue ($C_{16}H_{18}ClN_3S{\cdot}3H_2O$) supplied by BDH Chemicals (Middle East Dubai, UAE) and was used for experimental work as received. The standard solution of MB (1,000 mg/L) was prepared by mixing 1 g of MB into distilled water (1,000 mL) and was diluted from 5–25 mg/L. λ_{max} = 665 nm was determined by following the procedure described earlier [29].

2.2. Preparation of VG leaves powder (adsorbent)

The VG leaves were collected and rinsed thoroughly using purified water, de-hydrated at ordinary temperature, crushed and ground into fine powder by means of grinder and passed through the micro-sieves (70 netting size) before using in experiments. The 10 g of VG leaves powder was added in 100 mL of 0.1 M NaOH for the preparation of base modified VG leaves. The stirring of the mixture was carried out by using a magnetic stirrer for 24 h. Then the filtration and washing of powder were performed with distilled water and kept overnight in an oven for drying at 70°C for further use.

2.3. Characterization of adsorbent

A scanning electron microscope was employed for the characterization of powdered VG leaves. The exterior morphology of VG foliage fine particles was observed before and after adsorption experiments. The surface morphologies of before and after adsorption of MB onto VG leaves showed clear differences as shown in (Figs. 1a and b). The after adsorption microphotograph (Fig. 1b) clearly showed that MB was adsorbed upon the rough surfaces of an adsorbent.

The SEM photographs of base modified VG leaves showed the porous surface morphology before the adsorption of MB. These pores were filled or covered by MB dye after adsorption and a smooth surface is observed after adsorption (Figs. 1c and d).

2.4. FTIR analysis

The external functional groups of VG leaves prior and subsequent to adsorption were determined by FTIR analysis. The recording of the spectrum was carried out from 4,000 to 500 cm^{-1}. Prominent peaks for before adsorption observed were 3,515 and 2,968 cm^{-1} indicating –OH group and C–H stretching mode of aliphatic compounds respectively. The prominent peak at 1,739 cm^{-1} was that of C=O and peaks between 1,365 to 1,216 cm^{-1} were attributed to C–H, NH, C–H, and OH groups (Fig. 2a). All these peaks were absent in the after adsorption IR spectrum of adsorbent (Fig. 2b). Most probably, these groups were involved in bonding with methylene blue and were not noted in the after adsorption IR spectrum. FTIR results showed that functional groups such as carboxyl, alkene and hydroxyl take part in dye binding.

The base modified VG leaves IR spectrum represented the same characteristics as of raw VG leaves with some minor changes or some variable intensities in the bands. Such as 3,515 cm^{-1} reduced to 3,384 cm^{-1}. The peak at 2,968 cm^{-1} is due to C–H stretching vibrations which disappeared after modification of VG leaves. The peaks present in 1,500–1,200 cm^{-1} region may be of –NH, O–C–H, C–C–H and C–OH functional groups [29]. At 877 and 848 cm^{-1}, the bending vibrations are clearly observed in the base modified VG leaves spectrum, which is absent in the raw VG leaves spectrum (Fig. 2c and d).

2.5. Thermal gravimetric analysis (TGA)

TGA was conducted using V 4.5A TA, SDT Q600 V 20.9. The thermogram was drawn between temperature and mass loss as shown in Fig. 3. Initially, the mass loss was because of vapor loss, dehydration, chemical decomposition, and sublimation [30] The mass deficit (%) obtained through thermogram remained 10.61%, 22.71%, 83.94%, and 97.16% at different temperatures 100°C (moisture contents), 250°C (organic matter), 470°C (loss of hydroxyl) and 692°C (decarbonation), respectively. Two phases were observed according to DSC analysis. The first phase had negative peaks and weight loss was observed because of the evaporation of various volatile compounds and moisture contents [31]. The energy is consumed in the drying and evaporation of volatile compounds so it showed an endothermic reaction

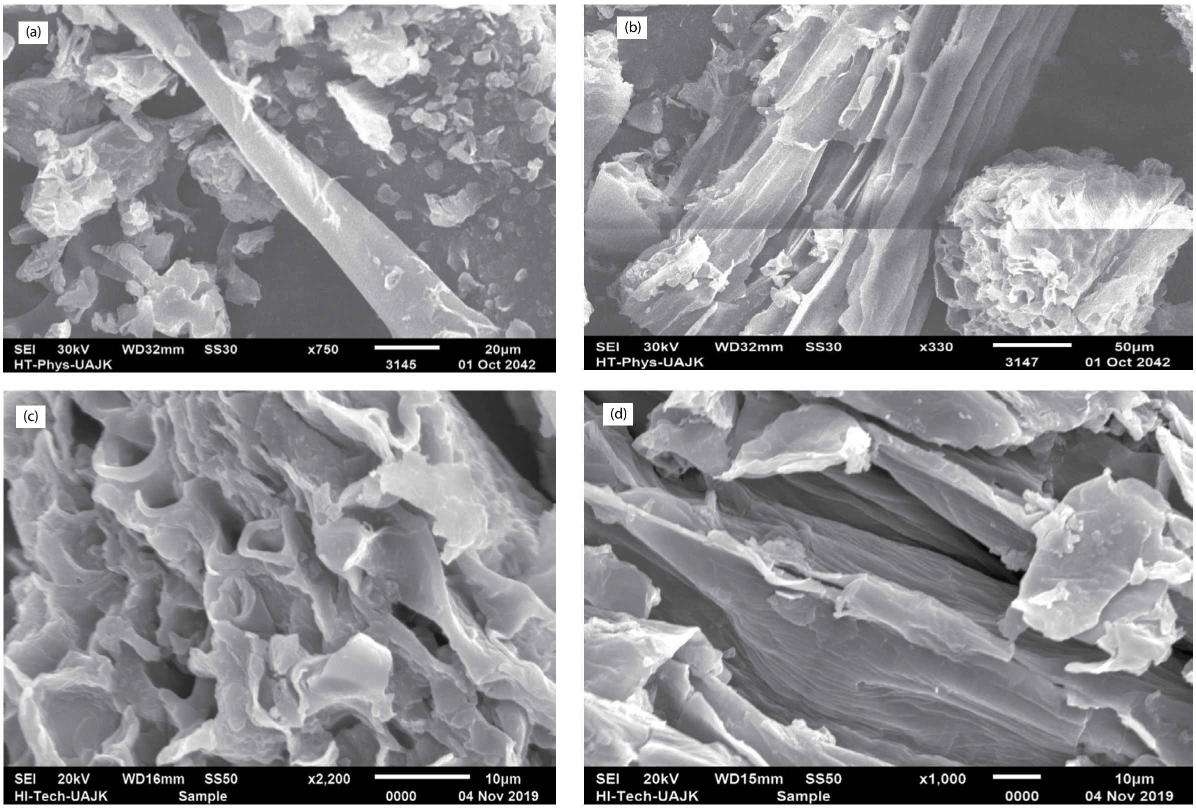

Fig. 1. (a) Before adsorption SEM analysis of VG leaves powder, (b) after adsorption SEM analysis of VG leaves powder, (c) base modified before adsorption SEM analysis of VG leaves powder, and (d) base modified after adsorption SEM analysis of VG leaves powder.

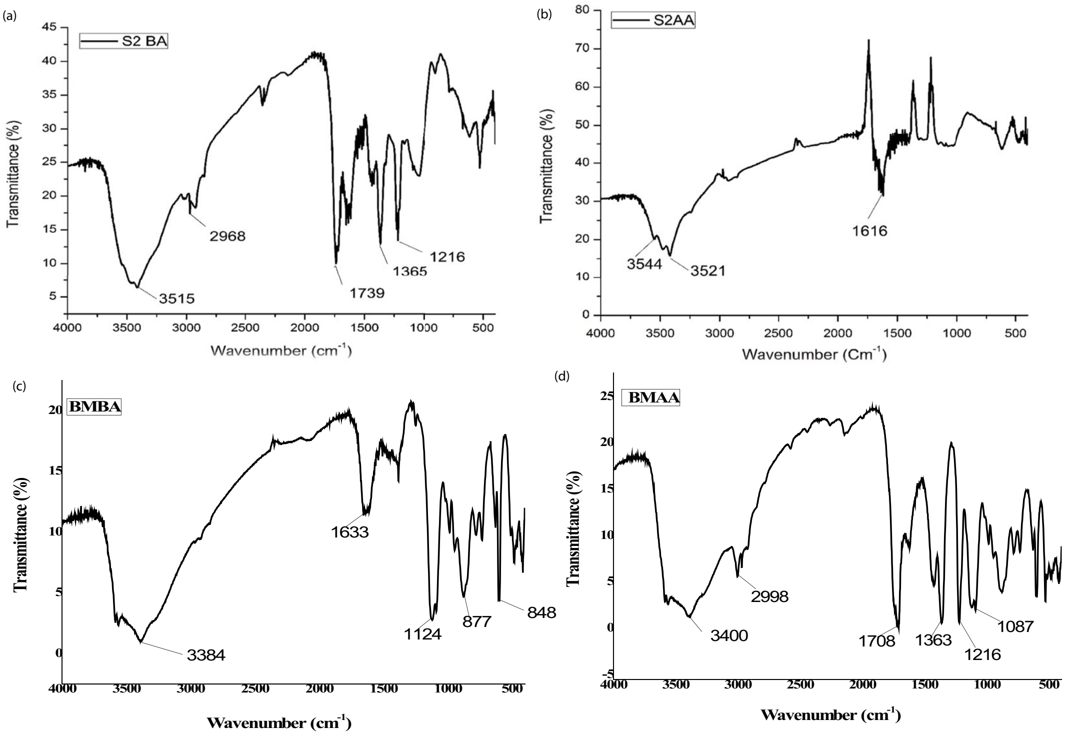

Fig. 2. (a) Before adsorption IR analysis spectra of VG leaves, (b) after adsorption IR analysis spectra of VG leaves, (c) base modified before adsorption IR analysis spectra of VG leaves, and (d) base modified after adsorption IR analysis spectra of VG leaves.

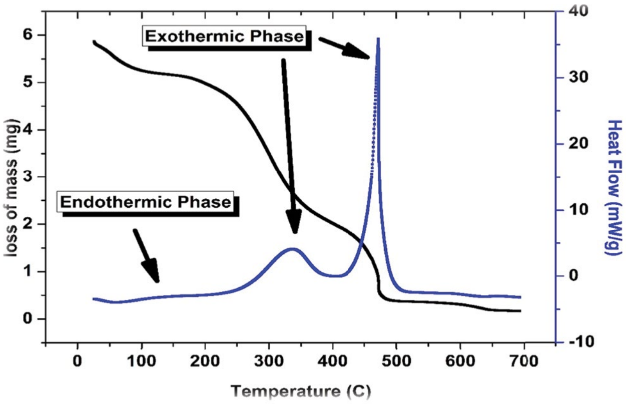

Fig. 3. Plot of TGA and DSC analysis.

below 270°C. The second phase started above 270°C where there was a faster loss of mass because lignin, hemicellulose and cellulose decomposed and this decomposition reaction was exothermic. The decomposition of biomass components at a variable temperature of 200°C–260°C, 240°C–350°C, and 280°C–500°C are hemicellulose, cellulose, and lignin, respectively, showed exothermic reaction [32].

2.6. Physical properties of the adsorbent

The textural characterization of VG using N_2 adsorption at 77 K was performed on a Quantachrome Novawin instrument (V. 11.04). The surface area was found to be 20.780 m^2/g, pore diameter 30.468 nm and pore density 0.099 cc/g. Moreover, the moisture content of the dried adsorbent (VG) was obtained using Eq. (1).

$$\text{Moisture contents} = \left(\frac{W_i - W_f}{W_i}\right) \times 100 \tag{1}$$

where the preliminary and final adsorbent weight (g) in the aforementioned equation is denoted by W_i and W_f respectively. The moisture content was found by 1.82% (Table 1).

2.7. Desorption studies

Different molar solutions of NaOH, HCl, KCl and distilled H_2O were utilized as desorbing agents. The 50 mL solution of MB (25 mg/L) and 0.15 g of adsorbent were treated for 60 min. Then the adsorbent (MB loaded) was stirred with the above-mentioned desorbing agents (25 mL) for 2 h. The dye concentration desorbed was determined and desorption percent was calculated by the following Eq. (2)

Table 1
Physical properties of *Viburnum grandiflorum*

Adsorbent			*Viburnum grandiflorum*
BET analysis		Physical properties	
Surface area	20.780 m^2/g	Moisture content	1.82%
Pore diameter	30.468 nm	Bulk density	0.417 g/cm^3
Pore volume	0.099 cc/g		

$$\%\text{Desorption} = \frac{m_d}{m_a} \times 100 \tag{2}$$

where m_d (mg/L) desorbed and m_a (mg/L) adsorbed amount of MB.

2.8. Batch equilibrium and kinetic studies

Batch adsorption was investigated by mixing 0.15 g VG in a 50 mL dye solution in three different conical flasks (250 mL). These flasks were heated at 293, 303, 313, and 323 K by using trembling hotplates covered with aluminum foil. Then these mixtures were filtered and absorbance of filtrates was carried out by UV-Visible spectrophotometer. The equilibrium concentrations of samples were calculated by employing Beer's Lambert law and adsorption capacity was estimated by the following relation.

$$q_e = \frac{\left(C_0 - C_e\right)V}{W} \tag{3}$$

where C_0 preliminary and C_e are the equilibrium concentrations of MB (mg/L) and (m) signifies adsorbent quantity in (g) while V denotes the solution's volume (L). The removal efficiency was attained by applying the following equation [33].

$$\%R = \frac{\left(C_0 - C_e\right)}{C_i} \times 100 \tag{4}$$

The equilibrium data analysis was carried using Langmuir, Freundlich and Temkin isotherm [34]. Langmuir isotherm is expressed as:

$$\frac{C_e}{q_e} = \frac{1}{Q_0 b} + \left(\frac{1}{Q_0}\right) C_e \tag{5}$$

The factor Langmuir isotherm was expressed as:

$$R_L = \frac{1}{1 + bC_0} \tag{6}$$

where the initial concentration of adsorbate (MB) is represented by C_0 (mg/L). The nature of adsorption can be estimated by R_L value; linear if ($R_L = 1$), un-favourable ($R_L > 1$), favourable ($0 < R_L < 1$) or irreversible ($R_L = 0$).

The non-linear equation for Langmuir can be expressed as:

$$q_e = \frac{q_m b C_e}{1 + bC_e} \tag{7}$$

The empirical isotherm describing a heterogeneous system is called as a Freundlich model as given below:

$$\ln q_e = \ln K_F + \frac{1}{n} \ln C_e \tag{8}$$

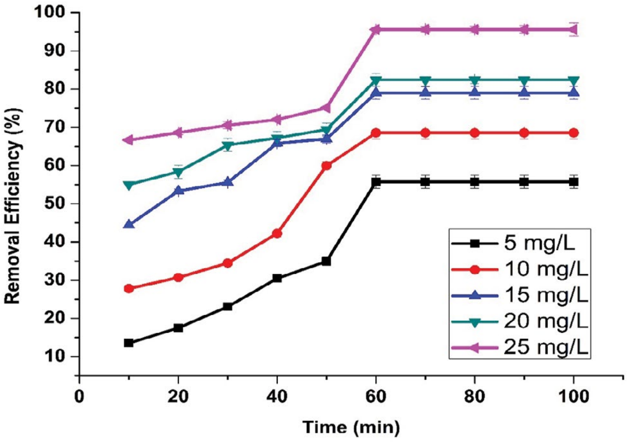

Fig. 4. Change in removal efficiency with time.

The Freundlich constants in the above equation are denoted by adsorption intensity (n) and adsorption capability K_F (mg/g (L/mg)$^{1/n}$).

Non-linear equation for Freundlich isotherms is written as:

$$q_e = K_F C_{\text{eq}}^{1/n} \tag{9}$$

The equation for the Temkin isotherm model is represented as:

$$q_e = B \ln A + B \ln C_e \tag{10}$$

where $RT/b = B$ which is constant for the heat of adsorption, b = Temkin constant of the heat of adsorption (J/mg), T = absolute temperature (K) and A = Equilibrium constant for maximum binding energy (L/g).

The thermodynamic parameters (such as entropy change ($\Delta S°$ J/K mol), enthalpy change ($\Delta H°$ kJ/mol and free energy change ($\Delta G°$ kJ/mol), were determined by using different equations:

$$\Delta G = -RT \ln K_c \tag{11}$$

$$\ln K_c = \frac{-\Delta G°}{RT} = -\frac{\Delta H°}{RT} + \frac{\Delta S°}{R} \tag{12}$$

where T for temperature in Kelvin, the K_c for equilibrium constant and R indicates gas constant (8.314 J/K mol).

3. Results and discussion

3.1. Effect of contact time

The MB solution (5–25 mg/L) was added in a conical flask (250 mL) with biosorbent dosage of 0.15 g for measuring the contact time effect by changing the stirring period from 10–100 min. UV-Visible spectrophotometer was employed for evaluating absorbance of the resulting filtrates and then equilibrium quantities were also finalized for estimating the adsorption capability and obliteration efficiency by employing relations three and four. The dye uptake capacity and percentage efficiency were started to accelerate by raising the contact time from 10 min to 1 h and then stayed persistent with time. The obliteration efficiency stayed in the extent of 55.73%–95.59% for samples containing the initial amount of 25 mg/L. By increasing contact time the adsorption capacity also increased (0.95–7.96) mg/g (Fig. 4). At initial contact time the active sites for adsorption are easily available and hence result in faster adsorption rate because of the process of diffusion from the solution to the active sites [35]. In similar reported studies, 130 and 150 min are the optimum contact time for the adsorption of MB onto wheat shells and phoenix tree leaves respectively were observed in previous studies [36]. The maximum adsorption capacity 7.96 mg/g was obtained in this study and comparison of previous studies have been also given in the Table 4.

3.2. Influence of varying initial concentration

Initial dye concentration (5–25 mg/L) were taken for studying the adsorption of MB onto VG leaves using 0.15 g/50 mL adsorbent in 250 mL conical flask, agitating for 60 min at 293 K and pH = 9. Then the filtration was carried out and UV Vis-spectrophotometer was employed for absorbance measurement of residual mixtures. The equilibrium concentrations were calculated from the absorbance. By increasing the MB dye concentration from 5–25 mg/L, removal efficiency (55.73%–95.59%) and adsorption capacity (0.95–9.98 mg/g) were also increased. The changes in initial dye concentration give suitable dynamic forces in mitigating the hindrance of the mass of MB deviation between the solid and aqueous phase [37]. Therefore, the concentration of dye effects the removal efficiency. The literature survey indicated that any rise in the preliminary concentration of dyes, decreases the percent removal of dyes (50–500 mg/L) onto banana stalk, pomelo rind, *Citrus grandis* and *Ricinus communis* seed shells [38].

3.3. Effect of solution pH

The pH plays a vital role in the adsorption process and dye uptake capacity. The adsorption capacity increases (5.95–6.52 mg/g) for pH 4 to 9. The pH effect of the adsorption of MB onto VG leaves is shown in Fig. 5. The removal of MB was increased with an increase in pH (4–9). The maximum dye removal efficiency (97.81%) was attained at pH = 9. It is due to the attractive forces (electrostatic force) between the cationic dye (MB) and the negatively charged adsorbent surface. As the pH increases, the negatively charge on biomass (leaves) also increased. In addition at acidic or lower pH the rate of adsorption of MB onto biomass is low because of excessive H^+ ions and cations of dye available at active sites started competing with each other. There is a decrease in positively charged sites and an increase in negatively charged sites at alkaline medium or pH [35]. At the surface sites of VG, the number of positively charged ions increase at lower pH, because of electrostatic repulsion, the cationic dye adsorption is not favorable. Because of excess H^+ ions competing with the dye cations for the sites of adsorption on VG the MB adsorption decreases [35]. In the previous study, it was found that at basic or higher pH, the Wheat Shell surface particles become more negatively charged, which attracted the positively charged cations of methylene blue through electrostatic attractive forces [39].

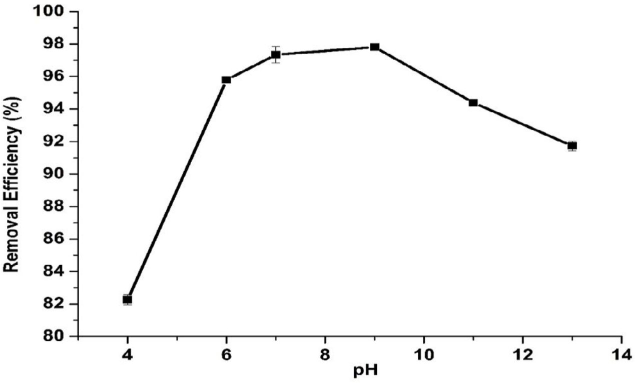

Fig. 5. Variable effects of pH on MB adsorption over VG (at an adsorbent dose 0.15 g, T = 298 K, t = 60 min and initial concentration 25 mg/L).

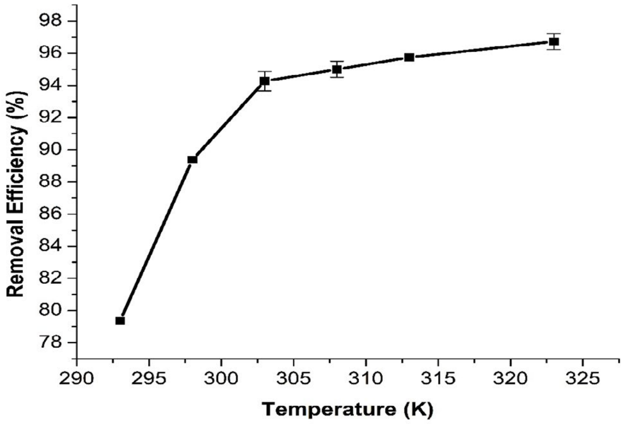

Fig. 6. Variable temperature effects on MB removal efficiency (at initial concentration 25 mg/L, pH = 9, t = 60 min and adsorbent dose 0.15 g).

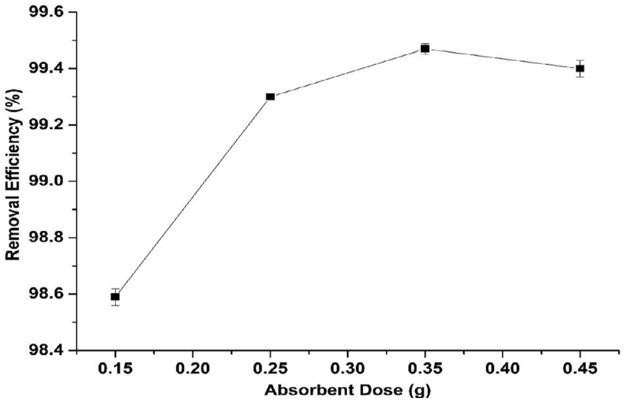

Fig. 7. Variable adsorbent dose effects on MB removal efficiency over VG (initial concentration 25 g/L, pH = 9, T = 298 K).

3.4. Effect of temperature

The adsorption of MB over VG was performed by using MB initial amount (25 mg/L), biosorbent dosage (0.15 g) and pH = 9 for studying the effect of temperature. The stirring of samples in electric thermostat shaker at temperature range 293–323 K was performed and then the samples were filtered. The equilibrium concentration was calculated by measuring the absorbance of the residual mixtures. The removal efficiency (79.37%–96.73%) and adsorption capacity (5.29–7.96 mg/g) increased with the increase in temperature (293–323 K) and its maximum was observed at 313 K (Fig. 6). The viscosity of the solution was dropped due to an increase in temperature so that adsorbate diffusion beyond the outermost surface border and also towards the adsorbent particles inner aperture was amplified resulting into a change in MB equilibrium capacity. The dye uptake capacity increase with increasing temperature showed the endothermic process. It might be because of the increase in mobility of molecules of dye and the number of active sites available for adsorption with the increasing temperature. The interaction between the number of increasing molecules and active sites at the surface of adsorbent increases because of sufficient energy gain by the molecules. The swelling of the internal structure due to a rise in temperature helps in the penetration of large dye molecules [40].

3.5. Effect of variable adsorbent dose

The deviations in adsorbent dosage influences were detected with 25 mg/L initial concentration of MB at contact time (60 min) and pH (9) at 298 K (Fig. 7). The varying dose (0.15 to 0.45 g/50 mL) of adsorbent was used and it was perceived that the obliteration capability of dye was improved from 98.59% to 99.4%. The rise in adsorption dosage between 0.15 to 0.45 g/ 50 mL has declined the adsorption capacity (from 6.57 to 2.2 mg/g), such behavior was because of the fact that at a high dose of adsorbent there was unsaturation of sorption sites during adsorption process [41]. On the contrary, the increase of sorbent dose has reduced the quantity of sorbed MB. The adsorption capability (q_e mg/g) on VG was declined (6.57 to 2.2 mg/g) for biosorbent dose fluctuating between 0.15 to 0.45 g. It is owing to the quantity of unsaturated vacant sites at the surface of adsorbent during adsorption. The unsaturated adsorption sites were further improved by an upsurge of adsorbent dose. The adsorption procedure was abnormally amplified by the greater dosage of adsorbent which has then lowered solutes of solution. The adsorption capacity (q_e) also declined due to the reduction of dye adsorption per unit adsorbent mass with an increase in adsorbent dosage [42].

3.6. Adsorption equilibrium

The adsorbate taken up by biosorbent and the remaining adsorbate concentration of adsorbate in the solution is described by the adsorption isotherm. The experimental data can be compared with the isothermal adsorption models at equilibrium [43]. The data was evaluated using Freundlich, Langmuir and Temkin isotherms. The Langmuir isotherm is suitable for the homogeneous systems, where adsorption takes place at the inner and outer surface of the adsorbent and most efficient for single layer adsorption. The linear Langmuir isotherm [44] (Eq. (5)) C_e (mg/L) is the concentration at equilibrium, q_e (mg/g), explains the adsorption of adsorbate per unit mass. The Langmuir constants (used in measuring potential) and the rate of adsorption are denoted by Q_0 and b, respectively. The C_e/q_e vs. C_e, exhibited straight lines (Fig. 8) for the adsorption of dye onto VG (Langmuir isotherm). The b and Q_0 Langmuir constants were analyzed and documented in Table 2. The R_L (Eq. (6)) is a dimensionless equilibrium constant also narrated by Saha and Dutta, 2009 [45].

In Eq. (6), adsorbate (MB) initial concentration is C_0 (mg/L). In current study, 0.065, 0.052, and 0.015 are R_L values at 303, 313, and 323 K respectively. This range of R_L values showed that VG is effective for adsorption of MB. The isotherm model (Freundlich) is expressed in Eq. (8) [46]:

In Eq. (8), q_e shows the amount of MB (mg/g) at equilibrium. K_F and n are Freundlich constants, K_F (mg/g (L/mg)$^{1/n}$) adsorption capacity of adsorbent and n showed that the adsorption process was satisfactory. The (1/n) slope value between 0 and 1 showed adsorption intensity and surface heterogeneity. Whereas, more heterogeneity was due to decreased slope value [47]. The planer outlines on the graph (Fig. 9) lnq_e vs. lnC_e had straight lines which showed that the MB adsorption is pertinacious to the Freundlich isotherm model (Table 3). The Temkin isotherm model was plotted between lnC_e vs. q_t (mg/g) (Fig. 10).

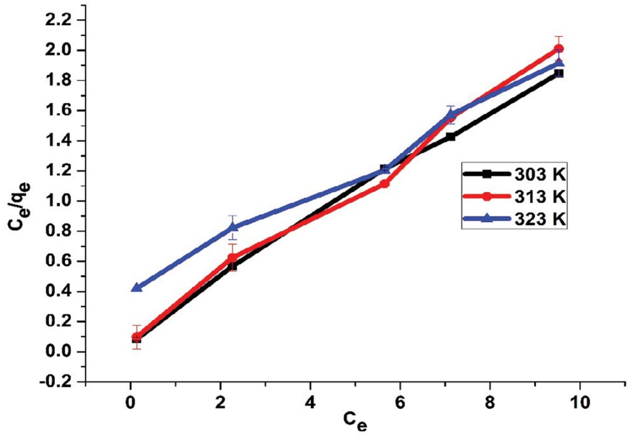

Fig. 8. Langmuir isotherm at various temperatures for MB adsorbed VG.

The non-linear isotherms models of Langmuir and Freundlich are employed for the adsorption of MB onto VG leaves. The isotherms parameters of linear and non-linear models differ from each other and are presented in Table 2. The R^2 values obtained from the non-linear form of Freundlich are less than linear isotherm. The comparison of both analysis delineated that the Langmuir isotherm is more conformed with correlation isotherm determination parameters than Freundlich.

The error analysis method sum of squared error (SSE) was performed for the assessment of the adequacy of the applied equation on the experimental data using the following relation.

$$\text{SSE} = \sum_{i=1}^{n} \left(q_{e,\text{calc}} - q_{e,\text{meas}} \right)^2 \tag{13}$$

The q_e (meas) representing the experimental and q_e (calc) is adsorption capacity value in (mg/g). The lower values of SSE best fitted with measured data. The SSE analysis of non-linear isotherm models have a close agreement with experimental data with the lower error shown in (Tables 2 and 3). The linear and non-linear analysis indicates R^2 is the best fitted with the Langmuir model.

3.7. Adsorption kinetics

The pseudo-first-order model by Lagergren [48] was employed in formulating the adsorption rate constant:

$$\log\left(q_e - q_t\right) = \log q_e - \left(\frac{K_1}{2.303} \right) t \tag{14}$$

Table 2
Adsorption isotherm model results for MB adsorbed VG

T (K)	Linear regression analysis											
	Langmuir constant					Freundlich constant				Temkin constant		
	Q_0 (mg/g)	b (L/mg)	R^2	R_L	SSE	K_F	N	1/n	R^2	B	K_t	R^2
303	9.34	0.57	0.99	0.065	17.53	40.96	2.12	0.47	0.84	1.465	2.112	0.91
313	7.04	0.72	0.99	0.052	5.076	10.00	3.77	0.26	0.99	0.775	3.017	0.99
323	2.55	2.46	0.99	0.051	6.335	3.74	2.27	0.43	0.99	1.232	1.806	0.93

Non-linear regression analysis							
	Langmuir constant				Freundlich constant		
T (K)	q_e	b	R^2	SSE	K_F	N	R^2
303	5.080	6.95	0.98	0.0059	24.32	2.91	0.78
313	5.910	5.910	0.98	1.276	28.44	2.64	0.98
323	4.95	3.845	0.98	0.018	7.99	1.98	0.89

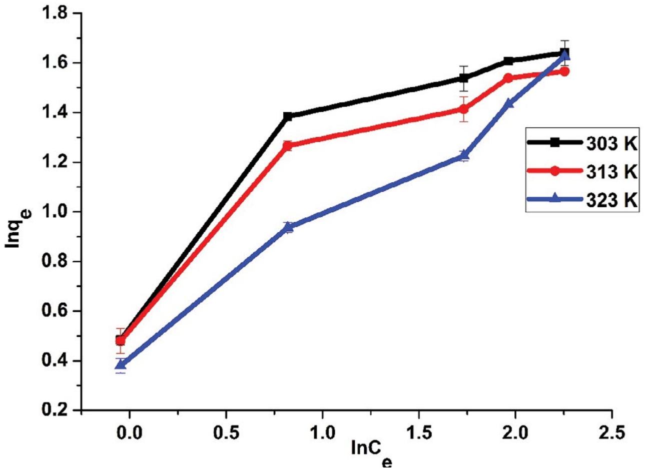

Fig. 9. Freundlich isotherm at various temperatures for MB adsorbed VG.

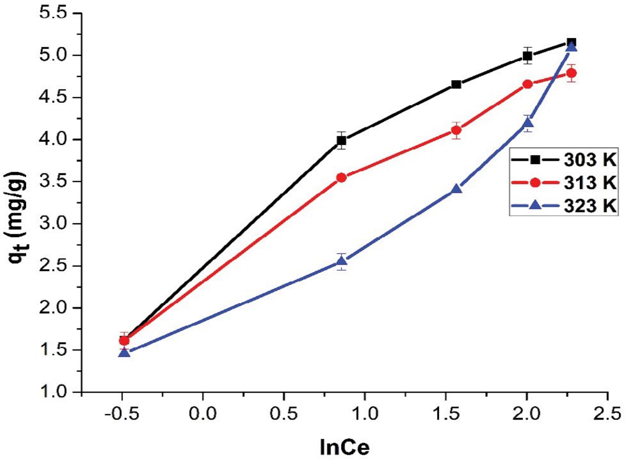

Fig. 10. Temkin isotherm at various temperatures for MB adsorbed VG.

where q_e (mg/g adsorption capacity at equilibrium) and q_t (mg/g) denote the adsorption capacity at time t (min). The graph of $\log(q_e - q_t)$ vs. time was utilized for calculating the K_1 and q_e for different MB concentrations (Table 3). The table shows that the isotherm data is most acceptable to the Lagergren [48] model with $R^2 \geq 0.99$ for different concentrations employed during the experiment. The kinetic data can also be calculated by the pseudo-second-order model (PSO) [49] using Eq. (15).

$$\frac{t}{q_t} = \frac{1}{k_2 q_e^2} + \left(\frac{1}{q_e}\right)t \tag{15}$$

The graph of t vs. t/q_t was employed to calculate equilibrium adsorption capability (q_e) and the pseudo-second-order constant (K_2). The kinetic data results of the pseudo-second-order model ($R^2 \geq 0.99$) showed the best fit of the model as compared to the pseudo-first-order (PFO) model and hence favored the adsorption of MB over VG leaves (Figs. 11 and 12). The Elovich model (EM) was also applied and is represented as:

$$q_t = a + b\ln t \tag{16}$$

The values of constants a and b were calculated from the plot of ln$t$ vs. q_t (Fig. 13), which gives a linear relationship [50]. Depending on the R^2 values, the adsorption kinetics of MB on VG followed the given order PSO > PFO > EM of kinetic models.

The rate-controlling step for the process of biosorption is determined by the intraparticle diffusion model. The Weber and Moris [47] plots were employed to accomplish the process of intraparticle diffusion. The Eq. (17) is given as:

$$q_t = K_i t^{1/2} + C \tag{17}$$

However, K_i (mg/g min$^{1/2}$) in the aforementioned equation designates the rate constant for intraparticle diffusion. The plot of $t^{1/2}$ vs. q_t showed two linear parts. The initial parts of the plot showed that the dye diffuses through the outer boundary layers that surround the adsorbent. The next part showed slow diffusion of dye into internal pores and equilibrium formation of dye at the adsorbent surface [51–54]. The multilinearity proposed that intraparticle diffusion is not a rate-limiting step for the adsorption process, but also involve the boundary layers of the biosorbent. The K_i and C were obtained from the slope-intercept of the plot (Fig. 14).

Table 3
MB removal results of adsorption kinetic

	Pseudo-first-order kinetic			Pseudo-second-order kinetic				Elovich model			Intraparticle diffusion model		
C_0 (mg/L)	q_e (mg/g)	K_1 (min^{-1})	R^2	q_e (mg/g)	K_2 (×10^3 g/(mg min))	R^2	SSE	a	b	R^2	K_i (mg/g min$^{1/2}$)	C	R^2
5	0.95	0.05	0.64	1.04	0.02	0.82	0.009	0.027	0.337	0.734	0.945	4.33	0.82
10	2.28	0.03	0.68	1.66	0.05	0.98	0.378	0.539	0.58	0.613	0.599	6.41	0.98
15	3.96	0.02	0.94	3.92	0.02	0.98	0.001	1.912	0.975	0.888	0.255	2.31	0.98
20	5.49	0.01	0.96	5.00	0.04	0.99	0.240	3.272	0.865	0.805	0.236	0.90	0.97
25	7.96	0.06	0.97	6.45	0.06	0.99	2.295	4.840	0.957	0.51	0.155	0.34	0.98

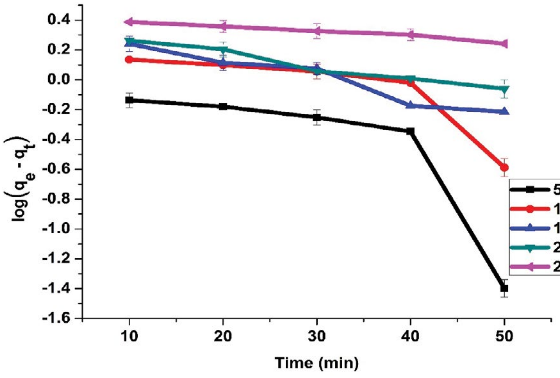

Fig. 11. Pseudo-first-order kinetics for MB adsorbed VG.

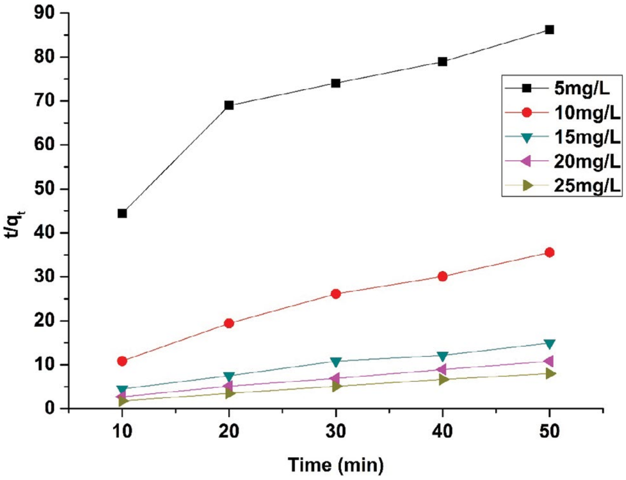

Fig. 12. Kinetics of pseudo-second-order of MB adsorbed VG.

Table 4
Comparative studies of adsorption capacities of adsorbents for MB removal

Adsorbents	q_m (mg/g)	References
Cashew net shell	5.31	55
Coarse grinded wheat straw	3.82	56
Neem leaf powder	3.67	57
Fine grinded wheat straw	2.23	56
Chitosan cross-linked (beads)	5.60	48
Coir pith carbon	5.87	49
Ficus palmata	6.89	29
Viburnum grandiflorum	7.96	This study

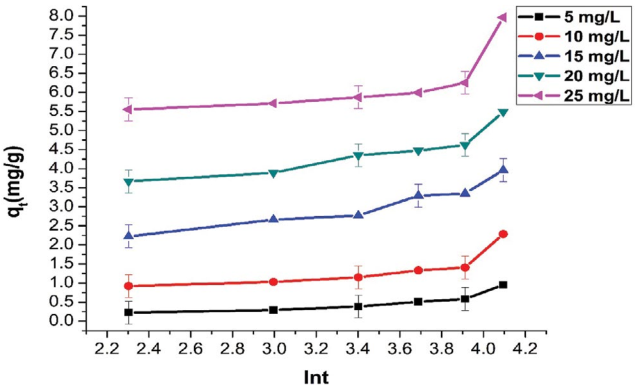

Fig. 13. Kinetics of Elovich model for MB adsorbed VG.

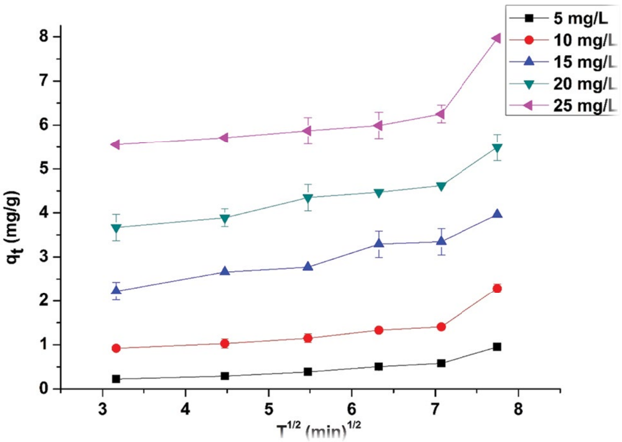

Fig. 14. Plot of intraparticle diffusion for MB removal at varying initial dye concentration.

Table 5
Thermodynamic results for MB adsorbed VG

Temperature (K)	ΔG° (kJ/mol)	ΔH° (kJ/mol)	ΔS° (kJ/mol)
303	–17.417		
313	–21.664	62.78	270.95
323	–23.212		

3.8. Thermodynamic parameters

The Gibbs free energy values for adsorption of MB onto VG at various temperatures (293, 303, and 313 K) were calculated to be (–17.417,–21.66, and–23.21 kJ/mol) and shown in Table 5. The lower negative values of Gibbs free energy showed spontaneous MB adsorption over VG. At higher temperatures, the adsorption process is more feasible due to the negative values of (ΔG°). The entropy factor role is significantly delineated by the upsurge process of adsorption with temperature. The ln$K$ vs. 1/T values were plotted for assessment of change of entropy and enthalpy (Fig. 15). The value of enthalpy change (ΔH°) was 62.78 kJ/mol, this positive value of MB adsorption on VG indicates that the reaction was spontaneous and endothermic in nature. The positive entropy change (ΔS°) values (270.28 J/K mol) represent the randomness at the solution of the adsorbate border during the adsorption process. More entropy is shown by the translational entropy gain by the dye molecule in the adsorption process. Many researchers found positive entropy change standards such as adsorbent Litchi chinensis-Acid Blue [55], Brazilian-pine fruit shell [56], *Bacillus subtilis*-MB [57], Reed-Basic yellow [58], *Azadirachta indica* leaf powder [59], *Citrus lemitta* and adsorbate methylene

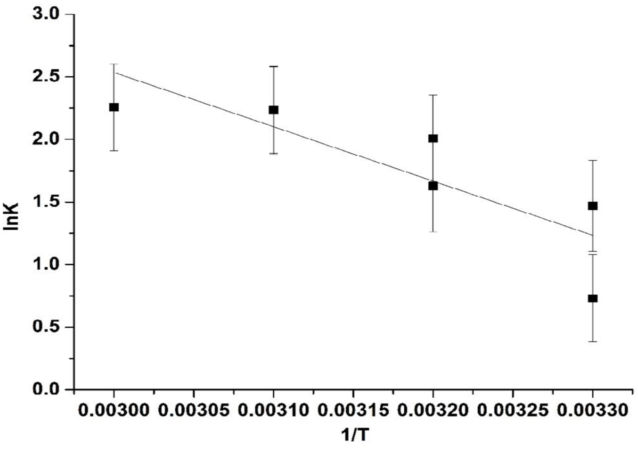

Fig. 15. Thermodynamic results for MB adsorbed VG.

blue [58], cross-linked chitosan/oil palm ash [60] and fly ash-MB [61].

3.9. Desorption

Different molar solutions of NaOH, HCl, KCl, and distilled H_2O were utilized as desorbing agents. It was found that the maximum percent desorption (25.78%) was carried out by HCl and hence designated as the most suitable desorbing agent for MB desorption from VG (Table 6). The molecules of MB migrate or diffuse from the solid phase into the liquid phase due to the concentration gradient and solvating power of the solvent (HCl in the present study). The adsorbent surface area might be another factor because the surface area and rate of desorption are directly related to each other [62].

4. Conclusions

The VG leaves (low-cost biowaste) material can be effectively and efficiently used for the MB removal from its aqueous solutions. According to textural analysis, pore diameter, pore volume and surface area were found to be 30.468 nm, 0.099 cc/g and 20.780 m²/g respectively. The decrease in dye uptake capacity was observed with the increasing biosorbent dose. Whereas the increase in contact time, pH, temperature and dye concentration increased the adsorption capacity. The rate of adsorption with a good correlation coefficient was compatible with pseudo-second-order kinetics. The data was observed best fitted with the Langmuir equation as compared to Freundlich isotherm. The pseudo-second-order model best described adsorption kinetics of methylene blue. The calculation of entropy ($\Delta S°$), enthalpy ($\Delta H°$) and Free energy ($\Delta G°$) changes are helpful for prediction of adsorption nature. The calculated values delineated the spontaneity of the adsorption process. The values of enthalpy and entropy changes of adsorption were calculated 62.78 and 270.95 kJ/mol respectively. The maximum removal efficiency was found to be 95.59% at 25 mg/L dye concentration for 60 min. The adsorption capacity was found to be 7.96 mg/g. The adsorption capacity and removal efficiency increased after modification of VG leaves with base (NaOH) and found to be 8.25 mg/g and 98% respectively. The MB loaded VG leaves can be best desorbed (25.78%) by using 0.1 M HCl. The VG leaves can be effective for the MB removal from aqueous solutions. The VG leaves (low-cost material) can be an alternative for dye removal in the treatment of wastewater instead of costly adsorbents.

Table 6
Different desorbing agents (MB loaded VG) % desorption results

Desorbing reagents	% Desorption
0.1 M HCl	25.78
0.1 M KCl	6.201
0.1 M NaOH	8.52
Distilled water	7.05

References

[1] R. Ayyappan, A.C. Sophia, K. Swaminathan, S. Sandhya, Removal of Pb (II) from aqueous solution using carbon derived from agricultural wastes, Process Biochem., 40 (2005) 1293–1299.

[2] S. Dawood, T.K. Sen, Removal of anionic dye Congo red from aqueous solution by raw pine and acid-treated pine cone powder as adsorbent: equilibrium, thermodynamic, kinetics, mechanism and process design, Water Res., 46 (2012) 1933–1946.

[3] Z. Yu, T. Qi, J. Qu, L. Wang, J. Chu, Removal of Ca (II) and Mg (II) from potassium chromate solution on Amberlite IRC 748 synthetic resin by ion exchange, J. Hazard. Mater., 167 (2009) 406–413.

[4] A.K. Meena, G. Mishra, P. Rai, C. Rajagopal, P. Nagar, Removal of heavy metal ions from aqueous solutions using carbon aerogel as an adsorbent, J. Hazard. Mater., 122 (2005) 161–170.

[5] T.K. Sen, S. Afroze, H. Ang, Equilibrium, kinetics and mechanism of removal of methylene blue from aqueous solution by adsorption onto pine cone biomass of *Pinus radiata*, Water Air Soil Pollut., 218 (2011) 499–515.

[6] V. Gupta, A.I. Suhas, V. Saini, Removal of rhodamine B, fast green, and methylene blue from wastewater using red mud, an aluminum industry waste, Ind. Eng. Chem. Res., 43 (2004) 1740–1747.

[7] W.T. Tsai, K.J. Hsien, H.C. Hsu, Adsorption of organic compounds from aqueous solution onto the synthesized zeolite, J. Hazard. Mater., 166 (2009) 635–641.

[8] N.M. Mahmoodi, B. Hayati, M. Arami, C. Lan, Adsorption of textile dyes on pine cone from colored wastewater: kinetics, equilibrium and thermodynamic studies, Desalination, 268 (2011) 117–125.

[9] L. Cui, C. Liu, G. Wu, Performance and mechanism of methylene blue biosorption on an orange peel, Environ. Technol., 29 (2008) 1021–1030.

[10] M. Sciban, M. Klasnja, B. Skrbic, Adsorption of copper ions from water by modified agricultural by-products, Desalination, 229 (2008) 170–180.

[11] R. Sivaraj, C. Namasivayam, K. Kadirvelu, Orange peel as an adsorbent in the removal of acid violet 17, Water Air Soil Pollut., 223 (2001) 5267–5282.

[12] T. Robinson, B. Chandran, P. Nigam, Removal of dyes from an artificial textile dye effluent by two agricultural waste residues, corncob and barley husk, Environ. Int., 28 (2002) 29–33.

[13] V. Vadivelan, K.V. Kumar, Equilibrium, kinetics, mechanism, and process design for the sorption of methylene blue onto rice husk, J. Colloid Interface Sci., 286 (2005) 90–100.

[14] V. Garg, R. Gupta, Y.A. Bala, R. Kumar, Dye removal from aqueous solution by adsorption on treated sawdust, Bioresour. Technol., 89 (2003) 121–124.

[15] P. Janos, H. Buchtova, M. Ryznarova, Sorption of dyes from aqueous solutions onto fly ash, Water Res., 37 (2003) 4938–4944.

[16] M. Visa, C. Bogatu, A. Duta, Simultaneous adsorption of dyes and heavy metals from multicomponent solutions using fly ash, Appl. Surf. Sci., 256 (2010) 5486–5496.

[17] N. Oladoja, C. Aboluwoye, Y. Oladimeji, A. Ashogbon, I. Otemuyiwa, Studies on castor seed shell as a sorbent in basic dye contaminated wastewater remediation, Desalination, 227 (2008) 190–203.

[18] R. Han, W. Zou, W. Yu, S. Cheng, Y. Wang, J. Shi, Biosorption of methylene blue from aqueous solution by fallen Phoenix trees leaves, J. Hazard. Mater., 141 (2007) 156–162.

[19] A.K. Rasheed, H. Tahir, F. Uddin, U. Hameed, Adsorption of methylene blue from aqueous solution on the surface of wool fiber and cotton fiber, J. Appl. Sci. Environ. Manage., 9 (2005) 29–35.

[20] B.A. Dar, A. Tahir, M. Arif, A. Wani, M. Farooqui, Lawn grass: an excellent and low-cost sorbent for the removal of Ni (II) ions from wastewater, Electron J. Environ. Agric. Food Chem., 11 (2012) 1259–2641.

[21] U. Kouakou, A.S. Ello, J.A. Yapo, A. Trokourey, Adsorption of iron and zinc on commercial activated carbon, J. Environ. Chem. Ecotoxicol., 5 (2013) 168–171.

[22] V. Rajeshwarisivaraj, V. Subburam, Activated parthenium carbon as an adsorbent for the removal of dyes and heavy metal ions from aqueous solution, Bioresour. Technol., 85 (2002) 205–206.

[23] B.A. Dar, A. Tahir, A. Wani, M. Farooqui, Isotherms and thermodynamic studies on adsorption of copper on powder of shed pods of *Acacia nilotica*, J. Environ. Chem. Ecotoxicol., 5 (2013) 17–20.

[24] K. Alau, C.E. Gimba, J.A. Kagbu, Removal of dyes from aqueous solution using neem (*Azadirachta indica*) husk as activated carbon, Arch. Appl. Sci. Res., 2 (2010) 456–461.

[25] P. Saha, Assessment on the removal of methylene blue dye using tamarind fruit shell as biosorbent, Water Air Soil Pollut., 213 (2010) 287–299.

[26] K. Kadirvelu, M. Kavipriya, C. Karthika, M. Radhika, N. Vennilamani, S. Pattabhi, Utilization of various agricultural wastes for activated carbon preparation and application for the removal of dyes and metals ions from aqueous solutions, Bioresour. Technol., 87 (2003) 129–132.

[27] A. Habib, M. Zahidul Hasan, M. Shajedur Rahman, S. Alam, Tuberose sticks as an adsorbent in the removal of methylene blue from aqueous solution, Pak. J. Anal. Environ. Chem., 7 (2006)112–115.

[28] S. Shakoor, A. Nasar, Removal of methylene blue dye from artificially contaminated water using *Citrus limetta* peel waste as a very low-cost adsorbent, J. Taiwan Inst. Chem. Eng., 66 (2016) 154–163.

[29] R. Fiaz, M. Hafeez, R. Mahmood, *Ficus palmata* leaves as a low-cost biosorbent for methylene blue: thermodynamic and kinetic studies, Water Environ. Res., 91 (2019) 689–699.

[30] B.T. Pelosi, L.K.S. Lima, M.G.A. Vieira, Removal of the Synthetic dye remazol brilliant blue R from textile industry wastewaters by biosorption on the macrophyte *Salvinia natans*, Braz. J. Chem. Eng., 31 (2014) 1035–1045.

[31] H. Yang, R.Yan, H. Chen, H. Dong, H.D. Lee, C. Zheng, Characteristics of hemicellulose, cellulose and lignin pyrolysis, Fuel, 86 (2007) 1781–1788.

[32] A. Marcilla, A. Gomez-Siurana, C. Gomis, E. Chapuli, M.C. Catala, F.J. Valdes, Characterization of microalgal species through TGA/FTIR analysis: application to *Nannochloropsis* sp, Thermochim. ACTA, 484 (2009) 41–47.

[33] B.H. Hameed, D.K. Mahmoud, A.L. Ahmad, Sorption of basic dye from aqueous solution by pomelo (*Citrus grandis*) peel in a batch system, J. Hazard. Mater., 158 (2008) 499–506.

[34] R. Ahmad, R. Kumar Adsorption studies of hazardous malachite green onto treated ginger waste, J. Environ. Manage., 91 (2010) 1032–1038.

[35] R. Ahmad, Studies on adsorption of crystal violet dye from aqueous solution onto coniferous pinus bark powder, J. Hazard. Mater., 171 (2009) 767–773.

[36] V.C. Srivastava, M.M. Swamy, I.D. Mall, B. Prasad, I.M. Mishra, Adsorptive removal of phenol by bagasse fly ash and activated carbon: equilibrium, kinetics, and thermodynamics, Colloids Surf., A, 272 (2006) 89–104.

[37] T. Santhi, S. Manonmani, Removal of methylene blue from aqueous solution by bioadsorption onto *Ricinus communis* epicarp activated carbon, Chem. Eng. Res. Bull., 13 (2009) 1–5.

[38] B.H. Hameed, Equilibrium and kinetic studies of methylene violet sorption by agriculture waste, J. Hazard. Mater., 154 (2008) 204–212.

[39] Y. Bulut, H. Aydın, A kinetics, and thermodynamics study of methylene blue adsorption on wheat shells, Desalination, 194 (2006) 259–267.

[40] D. Ozdes, C. Duran, H.B. Senturk, H. Avan, B. Bicer, Kinetics, thermodynamics and equilibrium evaluation of adsorptive removal of methylene blue onto natural illitic clay mineral, Desalination, 52 (2014) 208–18.

[41] D. Kavitha, C. Namasivayam, Experimental and kinetic studies on methylene blue adsorption by coir pith carbon, Bioresour. Technol., 98 (2007) 14–21.

[42] M. El-Guendi, Homogeneous surface diffusion model of basic dyestuffs onto natural clay in batch adsorbers, Adsorpt. Sci. Technol., 8 (1991) 217–225.

[43] F.A. Batzias, D.K. Sidiras, E. Schroeder, C. Weber, Simulation of dye adsorption on hydrolyzed wheat straw in batch and fixed-bed systems, Chem. Eng. J.,148 (2009) 459–472.

[44] I. Langmuir, Adsorption of gases on plane surfaces of glass mica platinum, J. Am. Chem. Soc., 40 (1918) 136–403.

[45] P. Saha, S. Dutta, Assessment on thermodynamics and kinetic parameters on the reduction of MB dye using fly ash, Desalination, 12 (2009) 219–228.

[46] H.M.F. Freundlich, Over the adsorption in solution, J. Phys. Chem., 57 (1906) 385–470.

[47] T.W. Weber, P. Chakkravorti, Pore and solid diffusion models for fixed-bed adsorbers, AIChE J., 20 (1974) 220–228.

[48] S. Lagergren, Zur Theorie Der Sogenannten Adsorption Geloester Stoffe, Kungliga Svenska Vetenskapsakad, Handl., 24(1898) 1–39.

[49] F. Haghseresht, G. Lu, Adsorption characteristics of phenolic compounds onto coal-reject-derived adsorbents, Energy Fuels, 12 (1998) 1100–1107.

[50] S.G. Muntean, A. Todea, M.E. Rădulescu-Grad, A. Popa, Decontamination of colored wastewater using synthetic sorbent, Pure Appl. Chem., 86 (2014) 1771–1780.

[51] R. Babuta, A. Popa, C. Pacurariu, E.S. Dragan, I. Lazau, Adsorption of some phenolic compounds on a new styrene-15% divinylbenzene copolymer functionalized with carboxylic groups volume, Chem. Bull. Politehnica Univ. Timisoara, ROMANIA, 60 (2015) 1.

[52] I.Y. Kimura, M.C.M. Laranjeira, V.T. Fávere, L. Furlan, The interaction between reactive dye-containing vinylsulfone group and chitosan microspheres, Int. J. Polym. Mater., 51 (2002) 759–768.

[53] O.M. Paşka, C. Păcurariu, S.G. Muntean, Kinetic and thermodynamic studies on methylene blue biosorption using corn-husk, RSC Adv., 107 (2014) 62621–62630.

[54] S.G. Muntean, A.Todea, S. Bakardjieva, C. Bologa, Oval of non-benzidine direct red dye from aqueous solution by using natural sorbents: beech and silver fir, Desal. Water Treat., 66 (2017) 235–250.

[55] A. Bhatnagar, A.K. Minocha, Assessment of biosorption characteristic of lychee peel waste for the removal of acid blue 25 dye from water, Environ. Technol., 31 (2010) 97–105.

[56] T. Calvete, E.C. Lima, N.F. Cardoso, J.C.P Vaghetti, S.L.P. Dias, F. Pavan, Application of carbon adsorbent prepared from Brazilian- pine fruit shell for removal of reactive orange-16 from aqueous solution: kinetic, equilibrium and thermodynamic studies, J. Environ. Manage., 91 (2010) 1695–706.

[57] A. Ayla, A. Cavus, Y. Bulut, Z. Baysal, C. Aytekin, Removal of methylene blue from aqueous solution onto *Bacillus subtilis*: determination of kinetic and equilibrium parameters, Desalination, 51 (2013) 7596–603.

[58] F. Boudrahema, F. Aissani-Benissada, A. Soualah, Removal of basic yellow dye from aqueous solution by sorption onto reed as an adsorbent, Desal. Water Treat., 54 (2014) 1–8.

[59] P.S. Kumar, R.V. Abhinaya, K.G. Lashmi, V. Arthi, R. Pavithra, V. Sathyaselvabala, S.D. Kirupha, S. Sivanesan, Adsorption of methylene blue dye from aqueous solution by agricultural waste: equilibrium, thermodynamics, kinetics, mechanism and process design, Colloid J., 73 (2011) 651–661.

[60] M. Hasan, A.L. Ahmad, B.H. Hameed, Adsorption of reactive dye onto cross-linked chitosan/oil palm ash composite beads, Chem. Eng. J., 136 (2008) 164–172.

[61] K.G. Bhattacharyya, A. Sharma, Kinetics and thermodynamics of methylene blue adsorption on neem (*Azadirachta indica*) leaf powder, Dyes Pigm., 65 (2005) 51–59.

[62] Momina, R. Mohd, I. Suzylawati, A. Anees, Optimization study for the desorption of methylene blue dye from the clay-based adsorbent coating, Water, 11 (2019) 1–13.